Modelling of Laser-Plasma Interaction on Hydrodynamic Scales: Physics Development and Code Validation

S. Weber,[1,2,*] G. Riazuelo,[2] P. Michel,[3,2] R. Loubère,[4] F. Walraet,[2] V. T. Tikhonchuk,[1] J. Ovadia,[5] and G. Bonnaud[6]

[1] *Centre Lasers Intenses et Applications, UMR 5107 CNRS - Université Bordeaux 1 - CEA, Université Bordeaux 1, 33405 Talence Cedex, France*

[2] *Département de Physique Théorique et Appliquée, CEA/DIF, BP 12, 91680 Bruyères-le-Châtel Cedex, France*

[3] *Laboratoire pour l'Utilisation des Lasers Intenses UMR 7605 CNRS - École Polytechnique - CEA - Université Paris VI, École Polytechnique, 91128 Palaiseau Cedex, France*

[4] *Los Alamos National Laboratory, Group T7, Los Alamos, NM 87544, USA*

[5] *CEA/DAM/CESTA/DEV/SIS, 33114 Le Barp, France*

[6] *CEA/DSE, 75752 Paris, France*

(Dated: May 28, 2003)

Abstract

The forthcoming laser installations related to inertial confinement fusion, LMJ (France) and NIF (USA), require multidimensional numerical simulation tools for interpreting current experimental data and to perform predictive modelling for future experiments. Simulations of macroscopic plasma volumes of the order of 1 mm^3 and laser exposure times of the order of hundreds of ps are necessary.

We present a new code for laser-plasma interaction which contains the relevant physics. The laser field is treated in a standard paraxial approximation in three dimensions. The plasma response is described by a single-fluid, two-temperature, fully non-linear hydrodynamical equations in the plane transverse to the laser propagation axis. The code also accounts for the dominant nonlocal transport terms in spectral form originating from a linearized solution to the Fokker-Planck equation. The simulations of interest lie with conditions as they are encountered in hohlraum plasmas in the case of indirect drive or the plasma corona for direct drive.

Recent experimental results on plasma-induced smoothing of RPP laser beams are used in order to validate the code.

short title: **Modelling of LPI**

number of manuscript pages: 14

number of figures: 6

PACS numbers: PACS: 52.40.Nk, 52.75.Di, 52.35.Mw

*Electronic address: `weber@celia.u-bordeaux.fr, stefan.weber@cea.fr`

I. INTRODUCTION

A detailed understanding of the interaction of a laser beam with a preformed underdense plasma is of outstanding interest in the context of inertial confinement fusion (ICF). Due to the complexity of the interaction process analytical models are only of limited use. Therefore numerical tools have to be conceived in order to be able to model laser-plasma interaction (LPI) (Berger et al. [2], Elisseev et al. [9], Hüller et al. [11], Myatt et al. [15], Pesme et al. [17]). Much work has been done for conditions where the plasma response can be taken to be linear and where the specific transport properties of laser-produced plasmas play less of a role (Elisseev et al. [9], Hüller et al. [11]). The forthcoming large-scale experiments for ICF in France (LMJ-Bordeaux) and the USA (NIF-Livermore) require codes which are capable to simulate the interaction process with a sufficient reliability in order to have the possibility to do predictive modelling of future experiments. This necessitates that the relevant physics is taken into account.

Ideally one would like to model the interaction process with first-principle tools such as Fokker-Planck or particle-in-cell (PIC) methods coupled to the full set of Maxwell's equations. Unfortunately these kind of calculations can at present only be done for microscopic plasma volumes. Hence a certain coarse-graining is necessary and the most promising approach at present would be to use some hydrodynamic model to describe the plasma. These kind of plasmas are characterized by the following aspects:

1. mixing of very disparate length-scales. The plasma response takes place at scales of the order or less than the laser wavelength λ_0 but the characteristic scale length of evolution of laser and plasma parameters amounts to several hundreds of laser wavelengths.

2. long time of simulations. The characteristic time of the plasma response varies in a very wide range from a few laser periods (in the case of Raman scattering) to thousands of laser periods for slower processes which involve the ion response.

3. large volume of simulations. The plasma volume to be treated in simulations is of the order of 1 mm^3. This is necessary for adequate description of speckle statistics, the backscattering processes and the nonlinear evolution of speckles.

4. the nonlinear aspect of plasma response can not be neglected. A simple ion-acoustic

wave (IAW) response for self-focusing and the three-wave model for stimulated scattering are of limited use for realistic laser parameters.

5. backscattering processes – the stimulated Raman and Brillouin scattering – have to be accounted for in a self-consistent picture of the interaction process. They are important for the energy balance in the target and for the effect of fast electrons on the pellet compression.

6. nonlocal aspect of the energy transport. For temperatures of several hundreds eV to a few keV and densities $\sim 0.1 n_c$ the transport properties can not be described by standard collisional equations. The transport is neither purely collisional (diffusive fluxes) nor collisionless (convective fluxes). The plasma is semi-collisional, a state which establishes itself whenever the characteristic mean-free path (mfp) for electron-ion collisions is of the order of the gradient scale lengths of the thermodynamic variables (density, temperature etc.). The consequence is a strongly modified pattern of temperature relaxation processes in the plasma. The issue of this so-called non-local transport (NLT) has been studied extensively in the literature (Alouani-Bibi and Matte [1], Brantov et al. [3], Bychenkov et al. [7, 8], Luciani et al. [13], Schurtz et al. [18]).

As a whole the contemporary LPI codes are complicated and difficult to validate. The most promising way is to have at hands simple and clean experiments which reduce the number of physical effects involved to a minimum and allow to deduce certain global characteristics (e.g. coherence times) which can be compared to the calculations. Once these codes have been validated in a convincing way, they can then be used to perform predictive modelling of future experiments (design experiments). Nonlinear hydrodynamic calculations are particularly time consuming and a full parallelization of such codes is mandatory.

In the following we are presenting a LPI code that has been developed recently on the base of the code PARAX (Riazuelo and Bonnaud [16]). The most important ingredients of this code and their implementation are briefly described as well as its first successfull validation.

II. PRESENTATION OF THE CODE

A. Electromagnetic module

The code is conceived to describe a propagation of a single laser beam in a weakly inhomogeneous, underdense plasma and the effects of ion density perturbations. For that it is not necessary to solve the full set of Maxwell equations. The wave equation for the electric field can be simplified in assuming that the propagation takes place dominantly in one given direction (here denoted as the z-direction). One assumes that the light which is linearly polarized in the x-direction, can be characterized by the frequency ω_0 and the wave vector $k_0 = (\omega_0/c)\sqrt{1 - n_{eo}/n_c}$ and that the amplitude is a slowly varying function of space and time:

$$\mathcal{E} = E(\mathbf{r}, t)\ \exp\left(\imath \int_0^z k_0(z')dz'\right) . \tag{1}$$

Then the laser amplitude E satisfies the paraxial equation (Feit and Fleck [10], Riazuelo and Bonnaud [16]) that can be written in the following form:

$$\left(2\imath\frac{\omega_0}{c^2}\partial_t + 2\imath k_0\partial_z + \imath\partial_z k_0 + \frac{2\nabla_\perp^2}{1+\sqrt{1+\nabla_\perp^2/k_0^2}} - \frac{\omega_0^2}{c^2}\frac{n_e - n_{eo}}{n_c} + \imath\frac{\nu_{ei}\omega_0}{c^2}\frac{n_{eo}}{n_c}\right) E = 0\,. \tag{2}$$

Here, n_e is the local plasma density and n_{eo} the intial plasma density, $n_c = m_e\epsilon_o\omega_0^2/e^2$ is the critical density. $\nabla_\perp^2 = \partial_x^2 + \partial_y^2$ is the Laplacian in the plane transverse to the direction of propagation, it describes the diffraction of the propagating laser beam. The factor $[1+(1+\nabla_\perp^2/k_0^2)^{1/2}]^{-1}$ takes into account deviations from the exact paraxial equation and allows to treat an opening angle of the order of 30°. Evidently it can be treated numerically only in an spectral approach (Feit and Fleck [10]). The term containing the electron-ion collision frequency ν_{ei} takes into account the laser energy losses due to inverse bremsstrahlung.

The paraxial approximation of the laser beam is based on several assumptions: $\partial_z \ll k_0$, $\partial_t \ll \omega_0$, and $\partial_z^2 \ll \nabla_\perp^2$. These conditions are supposed to be satisfied for the cases considered below.

B. Linearized plasma response

The simplest response of a plasma is due to the ponderomotive force which acts in the transverse direction. Quasi-neutrality is assumed and the response describes IAWs propa-

gating in the plane transverse to the propagation direction of the laser beam:

$$\left(\partial_t^2 + 2\gamma_s\partial_t - c_s^2\nabla_\perp^2\right)\ln\frac{n_e}{n_{eo}} = \frac{Z}{cm_in_c}\nabla_\perp^2\left(\wp I\right) . \tag{3}$$

Here, γ_s is a damping term and the intensity is given as $I = c\epsilon_o \mid E \mid^2 /2$. The characteristic speed of propagation of the density perturbations are determined by the acoustic velocity $c_s = \sqrt{(ZT_e + 3T_i)/m_i}$.

There are two modifications in this equation which go beyond the standard IAW equation. First is the logarithmic term on the left hand side instead of the linear density perturbation. This is an *ad hoc* attempt to extend the equation to the nonlinear case. It prevents unphysical negative values of n_e and reproduces the Boltzmann density depletion in the cavity. Second is the operator $\wp$ in front of the ponderomotive force on the right hand side. It is a spectral operator which takes account of non-local transport properties in the linear response regime (Brantov et al. [4]):

$$\wp_k = \frac{1}{2} + \frac{0.88Z^{5/7}}{(k_\perp\lambda_{ei})^{4/7}} + \frac{2.54Z}{1 + 5.5Z(k_\perp\lambda_{ei})^2}. \tag{4}$$

Here Z is the charge state of the ion, λ_{ei} is the mfp for electron-ion collisions and $k_\perp$ the perpendicular wave number.

C. Nonlinear hydrodynamics

For elevated intensities of the order of 10^{14} W/cm^2 and density perturbations above 10% the plasma response becomes nonlinear. In this case the simple IAW equation (3) has to be replaced by the full Euler-equations (Loubère [12]). The model used are the single-fluid (due to quasi-neutrality, $n_e = Zn_i$), two-temperature equations:

$$\partial_t n_i = -\nabla_\perp\cdot\left(n_i\mathbf{u}\right), \tag{5}$$

$$\partial_t(m_in_i\mathbf{u}) = -\nabla p_{tot}\,, \tag{6}$$

$$\partial_t(n_i\epsilon_i) = -\nabla_\perp\cdot\left(n_i\epsilon_i + p_i\right)\mathbf{u}\,, \tag{7}$$

$$\partial_t(n_e\epsilon_e) = -\nabla_\perp\cdot\left(n_e\epsilon_e + p_e\right)\mathbf{u}\,. \tag{8}$$

Here, $p_{tot} = p_e + p_i$ is the total plasma pressure, $p_e = (\gamma_e - 1)n_e\epsilon_e$ is the electron pressure and $p_i = (\gamma_i - 1)\left(n_i\epsilon_i - m_in_i\mathbf{u}^2/2\right)$ is the ion pressure, ϵ denotes the total energy which is related to the pressure by an equation of state for a given adiabatic coefficient $\gamma = c_p/c_v$. The electron inertia has been neglected in the electron equation of state.

As before the plasma response is taken in the transverse plane only. The hydrodynamics are solved in Lagrangian form on an unstructured triangular mesh using a discontinuous Galerkin-type approach which gives a high-precision numerics with little numerical diffusion and oscillations. In the above equations the coupling to the electromagnetic field (the ponderomotive force) as well as the transport terms are still missing - they are presented in the following section.

Figure 1 gives a simple visual impression of how linear and nonlinear response differ for elevated intensities. Amplitudes and frequency of self-focusing are clearly affected. This is especially important for density bumps which are severely overestimated in the linear model. Also the speed of propagation of density perturbations is no longer given by the ion-acoustic velocity, which is only correct in the initial stage, but will be larger. The dynamics of the problem changes fundamentally.

III. NON-LOCAL TRANSPORT

A. The properties of non-local transport

Using an approach based on the linearized version of the Fokker-Planck equation a set of transport coefficients in the context of semi-collisional plasmas has been derived by Brantov et al. [3], Bychenkov et al. [7]. As mentioned in the introduction, the transport coefficients are in general a strongly varying function of the product $k\lambda_{ei}$ where however the mfp is given in the real space. Figure 2 shows the dependence of the electron heat conductivity on the parameter $k\lambda_{ei}$.

The mathematical procedure of implementation of the nonlocal transport coefficients in the code is similar for each term. As an example let us consider at the following simplified heat equation comprising just the time dependence of the temperature due to the heat flux:

$$\partial_t T_e = \frac{2}{3n_e} \nabla \cdot (\kappa_e \nabla T_e) \,. \tag{9}$$

The electron heat conductivity κ_e is known in k-space only, hence the equation has to be evaluated in k-space itself. As one is above all interested in conditions where the semi-collisionality dominates one has that the gradient scale length is of the order of the mfp and therefore the conductivity does not vary much over the gradient. One can therefore assume κ_e to be constant locally and approximate the source $\nabla \cdot (\kappa_e \nabla T_e)$ as $\kappa_e \Delta T_e$. A further

approximation is not to evaluate the convolution sum in k-space as the approach is linearized anyway. Transforming to Fourier-space then amounts to the following replacement:

$$\nabla \cdot (\kappa \nabla T) \longrightarrow -k^2 \kappa_k T_k \,. \tag{10}$$

It has been assumed as well that the transport is isotropic in the transverse plane and that one can use the identification $k = \sqrt{k_x^2 + k_y^2}$. The change in temperature is then given as:

$$\delta T_e = \frac{2}{3} \frac{\Delta t}{n_e} \mathbf{F} \mathbf{T}^{-\mathbf{1}} \left[f_{nl}(k\lambda_{ei}) \alpha k T_k \right] \,. \tag{11}$$

Note that the coefficient $\alpha = n_e v_{Te}$ is given in real space. The function f_{nl} is a nonlinear function of $k\lambda_{ei}$ which can be decomposed as:

$$f_{nl}(k\lambda_{ei}) = g(Z) k\lambda_{ei} h(k\lambda_{ei}) \tag{12}$$

with $g(Z) = (3.26 + 13.6Z)/(4.2 + Z)$ giving the charge dependence. If the function h would be equal to 1 one would simply recover the standard expression for the collisional Spitzer-Härm conductivity: $\kappa = \kappa_{SH} = g(Z) n_e v_{Te} \lambda_{ei}$. In the general case the function is not equal to one and depends strongly on the collisionality of the plasma. It is possible to represent the function h as a harmonic mean between the strongly collisional and the collisionless state which gives a good approximation over the whole range of collisionality parameters:

$$h^{-1} = h_c^{-1} + h_{nc}^{-1} \,, \tag{13}$$

$$h_c^{-1} = 1 + \left(\frac{50 + 10Z}{12 + Z} X \right)^{0.9} \,, \tag{14}$$

$$h_{nc} = 0.11 \sqrt{Z}/X \,. \tag{15}$$

Here, $X = \sqrt{Z} k\lambda_{ei}$, h_c is the collisional contribution and h_{nc} is the non-collisional one.

B. Temperature relaxation in a hot spot

The effect of non-local transport can be easily appreciated by looking at a simple hot-spot relaxation due to the heat flux into the ambient medium (Senecha et al. [19]). Assuming a uniform temperature background of 700 eV, a local temperature perturbation of the form $T(r, t = 0) = T_0 \exp(-r^2/R^2) + 700$ eV is imposed. The speckle radius R is taken to be 7 μm and the perturbation amplitude is $T_0 = 70$ eV. For a density of $n_e = 0.1 n_c$ and a charge

state $Z = 5$ the resulting mfp is $\lambda_{ei} = 2.2$ μm and hence of the order of the characteristic gradient scale length of the perturbation R. For this case the above heat equation can be solved analytically and the relaxation times of the hot-spot for the collisional regime and the non-local transport regime can be calculated to give:

$$\tau_{SH} = \frac{3n_e R^2}{8\kappa_{SH}} = \frac{0.028R^2}{v_{Te}\lambda_{ei}\zeta} \approx 0.1 \text{ ps}\,, \tag{16}$$

$$\tau_{nl} = \tau_{SH}\left(1 + 10\sqrt{Z}k\lambda_{ei}\right)^{0.9} \approx 1.15 \text{ ps}\,. \tag{17}$$

Here, $\zeta(Z) = (0.24 + Z)/(4.2 + Z)$ takes into account the dependence on the charge state.

Obviously for the given, realistic, plasma conditions the relaxation times differ by a factor 10 which implies a strong variation in the plasma response to be expected.

The procedure outlined here for the evaluation of the non-local heat flux applies in exactly the same way for all the possible transport coefficients and associated transport terms.

C. Non-local Navier-Stokes equations

The resulting transport terms modify the Euler equations such that one obtains a non-local Navier-Stokes equations which can be written in the standard way as follows:

$$\partial_t n_i = - \nabla\cdot(n_i\mathbf{u})\,, \tag{18}$$

$$\begin{aligned}\partial_t \mathbf{u} = &- \mathbf{u}\cdot\nabla\mathbf{u} - \frac{1}{n_i m_i}\nabla p_{tot} - \frac{Z}{2cn_c m_i}\nabla I \\ &+ \frac{1}{n_i m_i}\nabla\cdot(\eta_i\nabla\mathbf{u}) + \frac{Z}{m_i}\nabla(\beta T_e) - \frac{Z}{cn_c m_i}\nabla\left(\xi_u + \frac{\beta}{3}\right) I\,,\end{aligned} \tag{19}$$

$$\begin{aligned}\partial_t T_e = &- \frac{2}{3}T_e\nabla\cdot\mathbf{u} - \mathbf{u}\cdot\nabla T_e + \frac{2}{3n_c c}\nu_{ei} I + \frac{1}{3n_c c}\partial_t I \\ &+ \frac{2}{3}T_e\nabla\cdot(\beta\mathbf{u}) + \frac{2}{3n_e}\nabla\cdot(\kappa_e\nabla T_e) - \frac{2}{3}\nabla\cdot\left(\frac{\kappa_e}{3n_e n_c c}\nabla I\right) \\ &- \frac{2}{3}\nabla\cdot\left(\frac{T_e}{m_e\nu_{ei}n_c c}\xi\nabla I\right)\,,\end{aligned} \tag{20}$$

$$\partial_t T_i = - \frac{2}{3}T_i\nabla\cdot\mathbf{u} - \mathbf{u}\cdot\nabla T_i + \frac{2}{3n_i}\nabla\cdot(\kappa_i\nabla T_i)\,. \tag{21}$$

In the above equations are some transport terms which are purely local such as the absorption due to inverse bremsstrahlung and the ponderomotive force term. The remaining terms going beyond those coming from the Euler equations involve the non-local transport coefficients which are only known in k-space. From the numerical point of view this implies that a

splitting scheme has to be employed in order to evaluate the transport. The transport is treated as a source for the Euler equations which is evaluated in Fourier space. The coupling therefore requires the transfer of quantities between the k-space on an Eulerian grid and the real-space on a Lagrangian grid. This leads to nontrivial numerical issues of coupling very different numerical schemes.

The non-local transport results from a linearization of the full Fokker-Planck equation and is nevertheless used in a nonlinear hydrodynamics. This is however justified as comparisons with kinetic calculations have shown that this approach remains valid even in the weakly nonlinear regime (Brunner and Valeo [5, 6]). The present model is one of several available in the literature. Comparison with other models (Alouani-Bibi and Matte [1], Schurtz et al. [18]) is needed to better understand their robustness and the limits of validity.

IV. VALIDATION OF THE CODE

Comparison with other codes and with experiments is an important part of the code development. The present code has already passed successfully certain tests. Here we present a comparison of the code with the results of a recent experiment on the plasma induced laser beam smoothing.

A. Experiment on the plasma-induced incoherence

The experiment looked at the time-resolved transmitted light of a RPP laser beam passing through a preformed plasma (Malka et al. [14]). An enhanced spatiotemporal smoothing of the laser beam was observed, Fig. 3. The plasma induced smoothing of a laser beam has been observed before albeit under very different conditions where self-focusing of the beam played an important role. In these experiments however the average power in a speckle was of the order of 3% of the critical power for self-focusing. An important parameter is the measured coherence time which in the experiment was of the order of 50 ps. The mechanism which was put forward to explain the loss of coherence induced by the plasma is multiple scattering. Even without self-focusing the presence of the ponderomotive force creates small density perturbations. The incident light is then scattered off these density perturbations which leads to an angular spreading of the light cone and to a loss of spatial and temporal

coherence. The characteristic time constant should therefore be given by the transit time for the speckle width. The random phase plate produced speckles with a characteristic radius of $2.8\,\mu$m. For a plasma temperature of $T_e = 250$ eV the acoustic velocity is $c_s = 0.06\,\mu$m/ps. The resulting acoustic transit time is therefore $t_{ac} = 50$ ps which agrees with the measured coherence time.

B. Calculations of the plasma-induced incoherence

In the following some calculations are presented which allow a code validation for the simplest configuration of the code: linear plasma response with non-local transport. This is justified as the experimental conditions were such that the level of backscattering was without significance and the laser intensity $\langle I \rangle \approx 6 \times 10^{13}$ W/cm^2 and plasma density ($n_e = 0.01 n_c$) such that the plasma response could be described by an IAW response. The results are summarized in Figs. 4, 5 and 6.

Figure 4 shows increasing fluctuations of the laser intensity as function of the plasma length implying an increasing loss of coherence. The variation of the laser intensity $\Delta I/\overline{I}$ was calculated as follows:

$$\Delta I = \sqrt{\langle (I(z,t) - I_0(z))^2 \rangle_t} \tag{22}$$

where $I_0(z) = \langle I(z,t) \rangle_t$ and $\overline{I} = \langle \langle I(z,t) \rangle_t \rangle_s$. The temporal and spatial average are defined as $\langle \ldots \rangle_t = T^{-1} \int I(z,t) dt$ and $\langle \ldots \rangle_s = L^{-1} \int I(z,t) dz$, respectively. Here, L is the plasma length and T the duration of the simulation.

The condition for multiple scattering to take place in the plasma can be shown to be [14]:

$$\left(1 + \frac{\rho_0^2}{\lambda_{ei}}\right)^2 \left(\frac{\langle I \rangle}{n_c c T_e} \frac{n_e}{n_c}\right)^2 k_0^2 L L_R > 1 \tag{23}$$

where $L_R = k_0 \rho_0^2$ the Rayleigh length. The term in the left bracket takes into account the effect of the non-local transport as the speckle radius $\rho_0 = 2.8\,\mu$m is of the order of the mfp $\lambda_{ei} = 4\,\mu$m.

The important parameter is the plasma length L which in the experiment was of the order of 2 mm. Even for very low intensities and densities laser beam smoothing can be achieved if the light interacts with a sufficiently long plasma. The calculation shows (see Fig. 5) clearly that the intensity profile is stationary the first one mm of the plasma before slow variations on the time scale of the ion-acoustic transit time set in. In a similar way Fig.

6 shows an arbitrary transverse intensity profile at the beginning of the plasma and after the light propagated through 2 mm of plasma. At the beginning of the plasma the profile does not change and remains strongly correlated for all times. In the contrast, the initial correlation has been completely destroyed at the end of the simulation box.

The physical effect taking place is the following sequence: the stationary random phase structure of the incident laser beam leads to non-stationary density perturbations and subsequently multiple scattering of the light takes place.

V. CONCLUSION

A code has been presented which was conceived to model the interaction of a paraxial laser beam with a preformed plasma in the context of inertial confinement fusion. The code structure requires the coupling of very different numerical modules which are optimized each for specific physics applications. This module coupling plus the fact that one operates in parallel on the Eulerian and Langrangian grids is non-trivial. The code has been optimized with respect to this coupling and has been validated qualitatively and quantitatively in the linear regime using experimental data on plasma-induced smoothing. The next step is the validation of the nonlinear plasma response for smoothing under conditions of strong self-focusing.

One has to be aware of the fact that a macroscopic calculations of LPI using a nonlinear plasma response are very demanding as far as CPU time is concerned. A linear plasma simulation which models roughly 1/8th of the LMJ beam requires of the order of one day on 40 processors at 833 MHz. Performing the same calculation using the fully nonlinear plasma response and the most relevant nonlocal transport terms adds a factor $10-20$ to the CPU time. Hence, the nonlinear macroscopic calculations can only be done on high-speed, massively parallel machines.

The present code can be considered a first but large step forward to a macroscopic modelling of laser-plasma interactions. The various minimal ingredients for a realistic physics basis have been presented. However, this is still far from what one needs in a long run. Missing components are for example: the backscattering processes (SRS and SBS), the expansion of the plasma in the parallel direction, a non-local transport model that would be valid in the strongly nonlinear regime.

Once the code has been decently validated by interpreting and reproducing present experimental data it can be used for predictive modelling of the forthcoming plasmas in the large-scale installations LMJ and NIF.

---

[1] Alouani-Bibi, F., Matte, J.-P. (2002). Phys. Rev. E **66**, 066414.

[2] Berger, R.L, Still, C.H., Williams, E.A., Langdon, A.B. (1998). Phys. Plasmas **5**, 4337.

[3] Brantov, A.V., Bychenkov, V.Yu., Tikhonchuk, V.T., Rozmus, W. (1996). JETP **83**, 716.

[4] Brantov, A.V., Bychenkov, V.Yu., Tikhonchuk, V.T., Rozmus, W. (1998). Phys. Plasmas **5**, 2742.

[5] Brunner, S., Valeo, E. (2000). Phys. Plasmas **7**, 2810.

[6] Brunner, S., Valeo, E. (2002). Phys. Plasmas **9**, 923.

[7] Bychenkov, V.Yu., Rozmus, W., Tikhonchuk, V.T., Brantov, A.V. (1995). Phys. Rev. Lett. **75**, 4405.

[8] Bychenkov, V.Yu., Novikov, V.N., Tikhonchuk, V.T. (1998). JETP **87**, 916.

[9] Elisseev, V.V., Ourdev, I., Rozmus, W., Tikhonchuk, V.T., Capjack, C.E., Young, P.E. (1997). Phys. Plasmas **4**, 4333.

[10] Feit, M.D., Fleck, J.A. (1988). J. Opt. Soc. Am. B **5**, 633.

[11] Hüller, S., Mounaix, Ph, Pesme, D. (1996). Physica Scripta **T63**, 151.

[12] Loubère, R. (2002). *Une méthode particulaire lagrangienne de type Galerkin discontinu. Applications à la mécanique des fluides et l'interaction laser/plasma.* PhD Thesis. Bordeaux University, Bordeaux.

[13] Luciani, J.F., Mora, P., Virmont, J. (1983). Phys. Rev. Lett. **51**, 1664.

[14] Malka, V., Faure, J., Hüller, S., Tikhonchuk, V.T., Weber, S., Amiranoff, F. (2003). Phys. Rev. Lett. **90**, 075002.

[15] Myatt, J., Maximov, A.V., Short, R.W. (2002). *Modelling laser-plasma interaction physics under direct-drive inertial confinement fusion conditions.* LLE Review, Quarterly Report, Univeristy of Rochester p. 93.

[16] Riazuelo, G., Bonnaud, G. (2000). Phys. Plasmas **7**, 384.

[17] Pesme, D., Hüller, S., Myatt, J., Riconda, C., Maximov, A., Tikhonchuk, V.T., Labaune, C., Fuchs, J., Depierreux, S., Baldis, H.A. (2002). Plasma Phys. Contr. Fusion **44**, B53.

[18] Schurtz, G.P., Nicolaï, Busquet, M. (2000). Phys. Plasmas **7**, 4238.

[19] Senecha, V.K., Brantov, A.V., Bychenkov, V.Yu., Tikhonchuk, V.T. (1998). Phys. Rev. E **57**, 978.

[20] Walraet, F. (2003). *Propagation et rétrodiffusion d'un faisceau laser lissé dans un plasma de fusion inertielle*. PhD Thesis. Ecole Polytechnique, Paris.

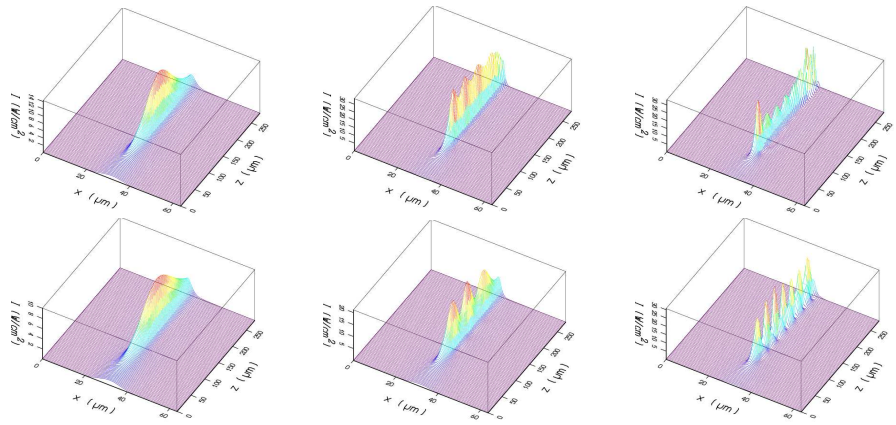

FIG. 1: Time evolution of a mono-speckle for $I = 6 \cdot 10^{14}$ W/cm^2, $n_e = 0.1 n_c$ and $T_e = 600$ eV. The snapshots are taken at 17.5, 22.5 and 30.0 ps. The upper row presents the results of the linear plasma response, the lower one the full nonlinear calculation. The nonlinear calculation includes only the ponderomotive force as coupling term, not the non-local transport.

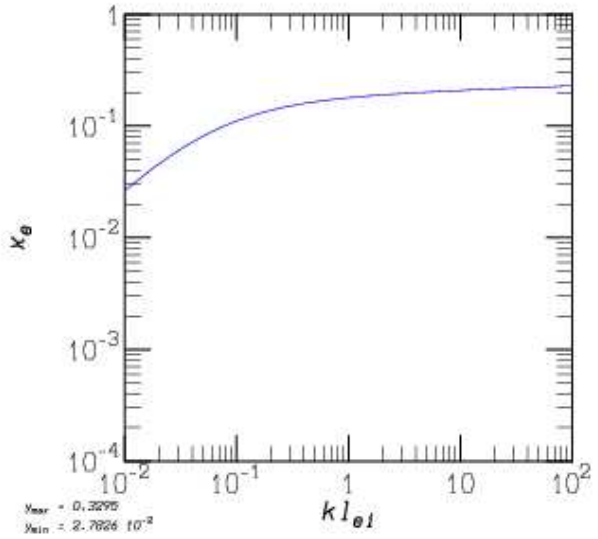

FIG. 2: The electron heat conductivity κ_e as a function of $k\lambda_{ei}$. For $k\lambda_{ei} \to 0$ one recovers the standard collisional transport value; the limit $k\lambda_{ei} \gg 1$ corresponds to the collisionless regime.

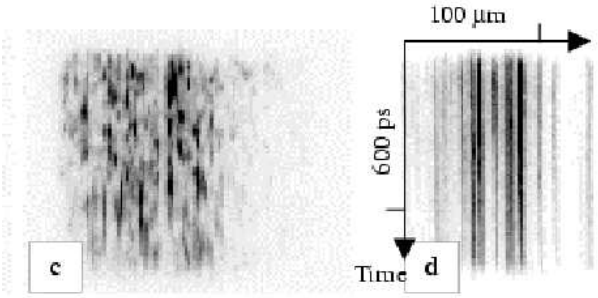

FIG. 3: Time resolved images of transmitted light using a RPP during 600 ps for 100 μm spatial extension. Left: with plasma, right: in vacuum.

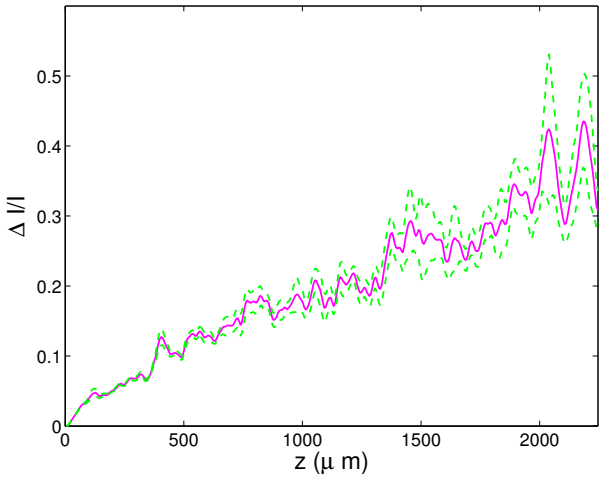

FIG. 4: The increasing fluctuations of the laser intensity as function of the plasma length. The curve is the mean value of 32 randomly chosen points in the transverse plane. The additional lower and upper curve give the mean square deviation of the values.

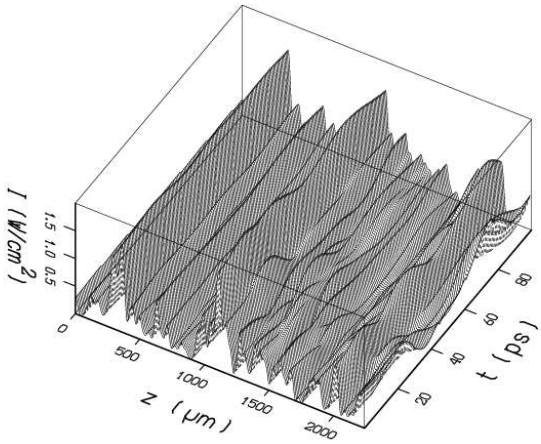

FIG. 5: Temporal evolution of the central intensity. The intensity depicted is in units of 1.85×10^{14} W/cm^2.

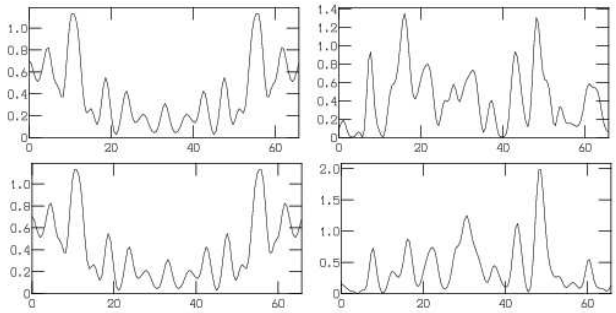

FIG. 6: The transverse intensity distribution for the RPP-case in an arbitrary point in the transverse plane. Left column: entrance of simulation box ($z = 0$); right column: end of simulation box ($z = 2240\,\mu$m). Upper row: at $t = 0$; lower row: at $t = 100$ ps.